

RESEARCH ARTICLE

OPEN ACCESS

## Experimental Study on Two-Phase Flow in Horizontal Rectangular Minichannel with Y-Junction

Agus Santoso\*, Rintaro Nagai\*, Akifumi Mori\*, Akimaro Kawahara\*, Michio Sadatomi \*

\*(Department of Advanced Mechanical Systems, Graduate School of Science and Technology, Kumamoto University, Kurokami 2-39-1 Chuo-ku, Kumamoto City 860-8555, Japan)

### ABSTRACT

An experimental study was conducted to investigate two-phase air-water flow characteristics, in horizontal rectangular minichannel with Y-junction. The width ( $W$ ), the height ( $H$ ) and the hydraulic diameter ( $D_H$ ) of the rectangular cross section for the upstream side of the junction are 4.60 mm, 2.50 mm and 3.24 mm, while those for the downstream side are 2.36 mm, 2.50 mm and 2.43 mm. The entire test section was machined from transparent acrylic block, so that the flow structure could be visualized. Liquid single-phase and air-liquid two-phase flow experiments were conducted at room temperature. The flow pattern, the bubble velocity, the bubble length, and the void fraction were measured with a high-speed video camera. Pressure profile upstream and downstream from the junction was also measured for the respective flows, and the pressure loss due to the contraction at the junction was determined from the pressure profiles. Two flow patterns, i.e., slug and annular flows, were observed in the fully-developed region apart from the junction. In the analysis, the frictional pressure drop data, the two-phase frictional multiplier data, bubble velocity data, bubble length data and void fraction data were compared with calculations by some correlations in literatures. In addition, new pressure loss coefficient correlations for the pressure drop at the junction has been proposed. Results of such experiment and analysis are described in the present paper.

**Keywords-** Minichannel, two-phase flow, Y-junction, bubble velocity, bubble length

### I. INTRODUCTION

Gas-liquid two-phase flow in mini-channels is a phenomenon seen in compact heat exchanger with phase changes, e.g., air conditioners, cooling devices in electronic equipments. In many arrangements it is necessary to divide the flow into two or more channel motivated by area restrictions or process requirements. There has been considerable interest recently in compact heat exchangers with mini- and micro-sized flow channels. These heat exchangers contain flow passages of various cross-sections (e.g., circular and rectangular), as well as various types of dividing tee junctions (e.g., branching and impacting) [1, 2]. Under two-phase flow conditions the behavior of the junction is complicated considerably by the structure of the gas-liquid mixture and, in particular, by its influence on the relative division of the two phases to the main and branch outlets, which becomes a parameter of great significance in the overall design of two-phase flow systems [3]. Flow distribution through the branches has to be investigated in order to design the system optimally.

Several investigations have been reported on two-phase flows in dividing tee junctions. For the case of impacting tees, a few studies have been reported in literatures (e.g., [1, 4, 5, 6, 7]). Elazhary and Soliman [2] investigated the single- and two-

phase pressure drops in a mini-size, horizontal, impacting tee junction with a rectangular cross-section (1.87-mm height x 20-mm width). The single-phase experiments were conducted using air or water in a wide range of Reynolds number, and the two-phase experiments using air and water at 200 kPa (abs) and room temperature for various inlet flow regimes. They reported the pressure loss coefficient for the single-phase flows was found to be dependent on Reynolds number in laminar flows ( $Re_{Dh} \leq 2000$ ), but independent of Reynolds number in turbulent flows ( $Re_{Dh} \geq 5000$ ). Four flow regimes were observed : bubbly, plug, churn, and annular flows. El-Shaboury et al. [8] conducted experiments for air-water flows in a horizontal impacting tee junction (37.8-mm i.d.) with equal-diameter sides at a system pressure of 1.5 bar nominally. They obtained phase-distribution and pressure drop and found that the phases did not distribute themselves evenly between the two outlets unless the mass split is equal.

For the case of branching tees, more than ten studies were reported by [9, 10, 11, 12, 13, 14, 15, 16, 17, 18, 19]. They studied the two-phase flow through a dividing T with 90 degree branch arms. However, there are few studies about the two-phase flows through a Y-junction. Ishiguro et al. [20] carried out experiments to separate gas from downward gas-liquid two-phase flows using a Y-

junction of poor wettability. The branch angle was 90 degree, and the inner diameters of the main pipe and two branches were 10 mm. One side of the channels downstream from the Y-junction was coated with repellent to change its wettability. Air and water were used as the working fluids. Guangbin et al. [21] reported the characteristics of gas-solid two-phase flows through a Y-shaped branch pipes (0.032-m i.d) with a fixed branch angle and the other adjustable branch angle. Micro-glass bead and millet particles with similar diameter but different density were used in this experimental system. As a result, the trend of solids mass ratio flowing in the adjustable branch and pressure drop on each branch pipe were analyzed to study flow distribution characteristics and resistance properties. It was found that the solids flow distribution and pressure drop for the two materials have similar trend and were significantly affected by the branch angle and gas velocity. Chen et al. [22] performed an experimental study of nitrogen-pure water two-phase flow splitting at microchannel junctions with the square cross-section of  $0.5 \times 0.5 \text{ mm}^2$ , and with five different branch angles varying from 30 to 150 degree. The inlet superficial velocities were varied from 0.8 to 21.3 m/s for the gas phase, and from 0.019 to 0.356 m/s for the liquid phase. Data analysis shows that the phase split at microchannel junctions depends strongly on inlet flow patterns. The liquid taken off from the branch did not decrease with increasing of the branch angle for all inlet flow patterns. Likewise, some researcher have studied computationally the flow through Y-junction such as, [23, 24, 25, 26].

The literature survey indicates that the research on two-phase flow in rectangular minichannel with Y-junction is limited. Therefore, the purpose of the present work is to investigate experimentally the two-phase flow in horizontal rectangular minichannel with the hydraulic diameter ( $D_H$ ) for the channel upstream from the junction 3.24 mm, and that for the downstream channel 2.43 mm. The high speed video technique was used to analyze the fluid dynamics of two-phase distribution at the junction. The experimental and the analytical results are compared with the data from previous studies and are presented in the present paper.

## II. EXPERIMENTS

A schematic diagram of the test facility used in the present study is shown in Fig. 1. As the test fluids, water was used for the liquid phase, and air for the gas phase. Pressurized air from a compressor pushed the water in a tank and supplies it to the test channel. Thus, no mechanical pump was used in the present experiment to avoid pulsation by the pump and also to avoid contamination by the pump. Figure 2 shows a schematic diagram of test channel with

branch placed on a horizontal plane. The branch angle was  $60^\circ$ . The test channel had a rectangular cross-section and made of transparent acrylic resin for visual observation. Table 1 shows the cross-sectional dimensions of the test channel on the width ( $W$ ), the height ( $H$ ) and the hydraulic diameter ( $D_H$ ). Those for the channel upstream from the junction (Upstream I) were 4.60 mm, 2.50 mm and 3.24 mm, while those for the channel downstream (Downstream II and Downstream III) were 2.36 mm, 2.50 mm and 2.43 mm. In Fig. 2, the port #1 was the liquid inlet port, while the port #2 and #3 were the gas inlet ports. Therefore, two phases were supplied through the section 1 as a gas-liquid mixer. The port #4 and #5 were the gas-liquid mixture outlet to individual separator tanks. Volume flow rate of air was measured with a flow meter (KEYENCE, FD-A10 AND FD-A1 depending on the flow rate range) within 2 %, while that of water with a flow meter (KEYENCE, FD-S) within 1 %.

In order to obtain accurate time averaged values of air and water flow rates and pressures, the output signals from the respective sensors were fed to a personal computer via A/D converter over 10 sec. at nominally 1 kHz.  $P_1$  to  $P_{15}$  are the pressure taps, and the pressure at  $P_4$  in Fig. 2 was measured with a gauge type pressure transducer (Yokogawa, FP101-L31-L20). The pressures at other pressure taps were determined from the difference in pressure between there and  $P_4$  tap measured with a differential pressure transducer (Validyne, DP15-32 and DP15-26 depending on the pressure range). The accuracy of the pressure measurement was within 4 Pa from a calibration test. The gas-liquid mixture discharged to each separator was separated. The air from the top of each separator was metered by a gas flow meter (SINAGAWA, DC-1C, 10 ~ 1100 L/h) before exhausting to the atmosphere. During the flow rate measurement, the water levels in the separator tanks were monitored to be in the respective constant levels. The water flow rate from the bottom of each separator tank was calculated by measuring the mass of water discharged per a enough measurement time. In the present experiment, the water flow rates of the two branch channels were adjusted to be equal each other as possible by changing the openings of two valves between the channel exit and the separator tank.

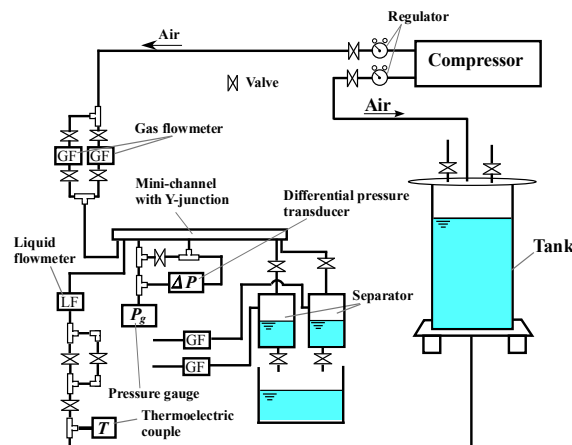


**Fig. 1 :** Test apparatus

Flow pattern was observed with a high-speed video camera (KEYENCE, VH-Z00R, frame rate : 1000 ~ 8000 frame/s, shutter speed 1/1000 ~ 1/8000s) in four observation area marked with broken circles in Fig. 2, and bubble velocity,  $u_G$ , in slug flow in the test channel was also measured. Furthermore, void fraction,  $\alpha$ , data was obtained by substituting the measured  $u_G$  and the gas volumetric flux,  $j_G$ , into  $\alpha = j_G/u_G$ . For single-phase water flow experiments, the ranges of Reynolds number ( $= \frac{\rho_L u_L D_H}{\mu_L}$ , where  $u_L$  is the mean velocity of water,  $\rho_L$  and  $u_L$  the density and viscosity of water) in the upstream channel was from 762 to 4661. For two-phase air-water flow experiments, the ranges of volumetric fluxes of the liquid and the gas were  $0.2 < j_L < 1.5$  m/s and  $0.2 < j_G < 5.0$  m/s.

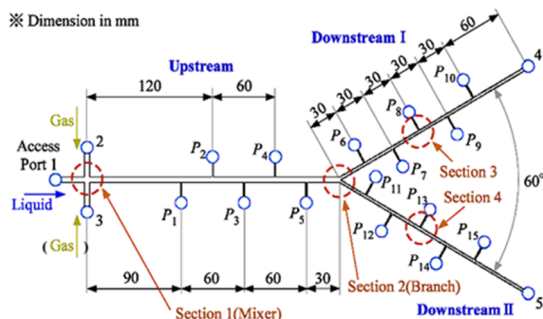


**Fig. 2 :** Test channel with Y-junction

**Table 1 :** Dimension of test channel cross section

	<b><i>W</i></b> [mm]	<b><i>H</i></b> [mm]	<b><i>D<sub>H</sub></i></b> [mm]
Upstream I	4.60	2.50	3.24
Downstream II, III	2.36	2.50	2.43

### III. RESULTS AND DISCUSSION

#### 3.1 Flow pattern

Figure 3 shows the flow pattern map in the present two-phase flow experiment. The ordinate and abscissa are the volumetric fluxes of water and

air. The flow regimes observed with a high-speed video camera covered in a range of  $0.2 \leq j_G \leq 5.0$  m/s and  $0.2 \leq j_L \leq 1.5$  m/s. Two flow regimes were observed, i.e., slug flow and annular flow under the present flow conditions.

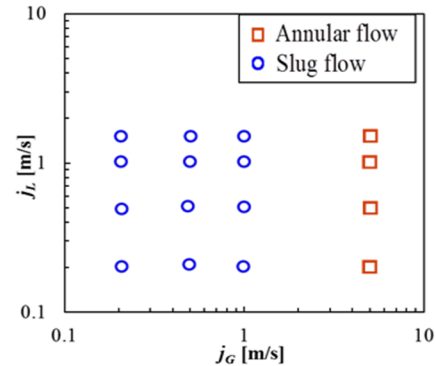
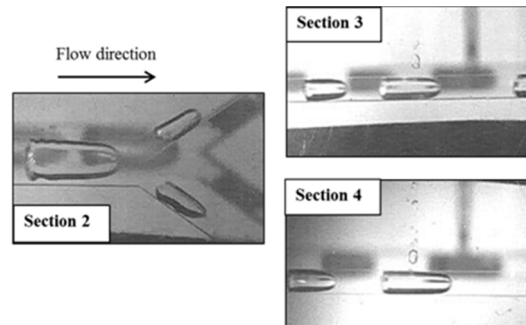
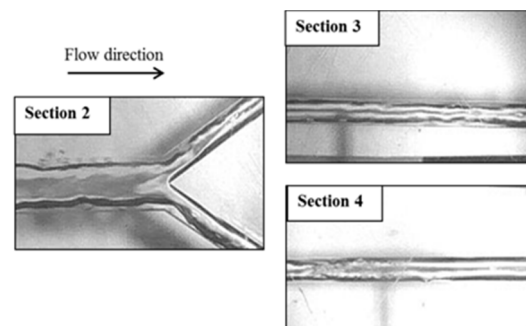


**Fig. 3 :** Flow pattern map in the present experiment

Figures 4 (a) and (b) show typical flows in the test channel, respectively for a slug flow at  $j_{G,I} = 0.5$  m/s,  $j_{L,I} = 0.5$  m/s and an annular at  $j_{G,I} = 5.0$  m/s,  $j_{L,I} = 0.5$  m/s. The flow regimes among upstream I, and downstream II and III are similar at all the experimental conditions.



**(a)** Slug flow ( $j_{G,I} = 0.5$  m/s,  $j_{L,I} = 0.5$  m/s)



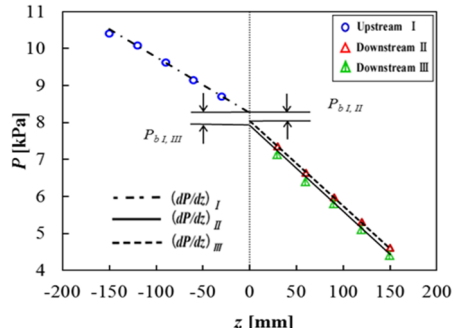
**(b)** Annular flow ( $j_{G,I} = 5.0$  m/s,  $j_{L,I} = 0.5$  m/s)

**Fig. 4:** Typical flows in the test channel

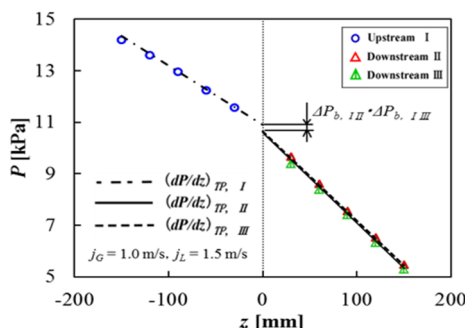
#### 3.2 Data reduction in pressure drop

Figures 5 (a) and (b) show typical pressure distributions for water single- and air-water two-phase flows upstream and downstream of Y-

junction. The ordinat is the gauge pressure, while the abscissa is the distance from the junction. There are five pressure taps, tap #1 to tap #5, for the upstream channel from the junction and the another ten taps, tap #6 to tap #15, for the downstream channel. The total pressure drop across the Y-junction,  $\Delta P_b$ , was determined by the extrapolations of the axial pressure profiles upstream and downstream from the junction, as shown in Figs. 5 (a) and (b).



(a) Single-phase flow ( $Re = 4700$ )



(b) Two-phase flow ( $J_G = 1.0 \text{ m/s}$ ,  $J_L = 1.5 \text{ m/s}$ )

**Fig. 5 :** Pressure distribution along the channel with Y-junction

In order to check the pressure measurement accuracy, the single-phase friction factors were determined from the fully developed pressure gradients upstream and downstream from the junction. Figs. 6 (a) and (b) show the Darcy friction factor data respectively for the channels upstream and downstream from the junction. The data are plotted against the Reynolds number, based on the hydraulic diameter. The present data in laminar flow region are compared with calculated curve by Shah and London [27] which is a function of aspect ratio,  $\alpha^*$  ( $= W/H$ ), for a rectangular channel :

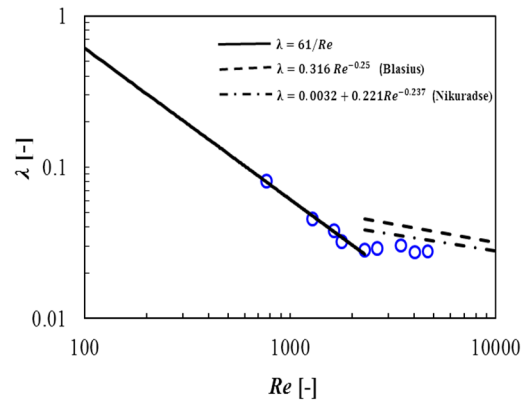
$$\lambda Re = 96(1 - 1.3553\alpha^* + 1.9467\alpha^{*2} - 1.7012\alpha^{*3} + 0.9564\alpha^{*4} - 0.2537\alpha^{*5}). \quad (1)$$

In addition, the data in turbulent flow are compared with familiar calculated curves by Blasius,

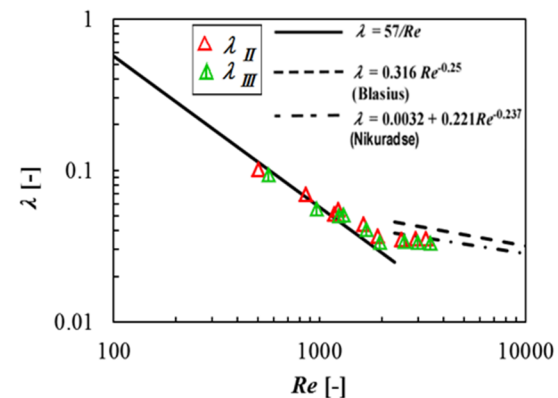
$$\lambda = 0.316 Re^{-0.25}, \quad (2)$$

and Nikuradse :

$$\lambda = 0.0032 + 0.221 Re^{-0.237}. \quad (3)$$



(a)  $\lambda$  vs.  $Re$  (Upstream I)



(b)  $\lambda$  vs.  $Re$  (Downstream II, III)

**Fig. 6 :** Single-phase friction factors in channels upstream and downstream from the junction

### 3.3 Pressure drop at Y-junction

The pressure drop at the Y-junction can be evaluated by the change in dynamic pressure between the flows in channels upstream and downstream from the junction. Since the two-phase flow energy per unit time is composed of two components as follows :

$$E_{TP} = \rho_G Q_G u_G^2 / 2 + \rho_L Q_L u_L^2 / 2. \quad (4)$$

Thus, the dynamic pressure, i.e., the flow energy/the total volume flow rate, is given by

$$P_{d,TP} = \rho_G \beta u_G^2 / 2 + \rho_L (1 - \beta) u_L^2 / 2. \quad (5)$$

Here  $\rho$ ,  $Q$  and  $u$  are the density, the volume flow rate and the mean velocity, and  $\beta$  the homogeneous void fraction defined as  $\beta = Q_G / (Q_G + Q_L)$ . Since the first term in the right hand side of Eq. (5) is much smaller

than the second term in bubble and slug flow regimes.  $P_{d,TP}$  can be approximated as :

$$P_{d,TP} = \rho_L(1-\beta)u_L^2/2 \quad (6)$$

Here,  $u_L (= j_L/(1-\alpha))$  is the mean liquid velocity and can be approximated as  $j_L/(1-\beta)$  because  $\alpha \approx \beta$  in the present experimental range as shown in Fig. 14, the last figure of the present paper. And then, Y-junction loss coefficients for single- and two-phase flows are defined as follows :

$$k_{SP, I\ II} = \frac{\Delta P_{bSP, I\ II}}{\rho_L u_{L,I}^2 / 2} \quad (7)$$

$$k_{SP, I\ III} = \frac{\Delta P_{bSP, I\ III}}{\rho_L u_{L,I}^2 / 2} \quad (8)$$

$$k_{TP, I\ II} = \frac{\Delta P_{bTP, I\ II}}{\rho_L(1-\beta_I)u_{L,I}^2 / 2} \quad (9)$$

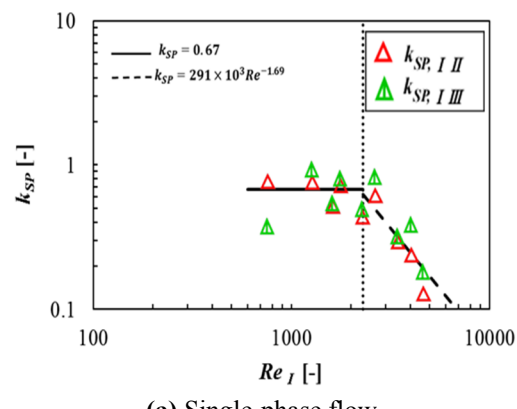
$$k_{TP, I\ III} = \frac{\Delta P_{bTP, I\ III}}{\rho_L(1-\beta_I)u_{L,I}^2 / 2} \quad (10)$$

Figures 7 (a) and (b) show the junction loss coefficient for single- and two-phase flows, respectively. In Figure 7 (a) both  $k_{SP, I\ II}$  and  $k_{SP, I\ III}$  data are simultaneously plotted. The abscissa is the Reynold number of the channel upstream from the junction. The vertical dotted line on the figure is the critical Reynold number ( $Re_I = 2300$ ), between laminar flow and turbulent flow. The junction loss coefficient in laminar flow region ( $Re_I < 2300$ ) is nearly constant, and it decreases with increasing of  $Re_I$  in turbulent flow region ( $Re_I > 2300$ ). Thus, the data for the single-phase flow in this study is correlated with

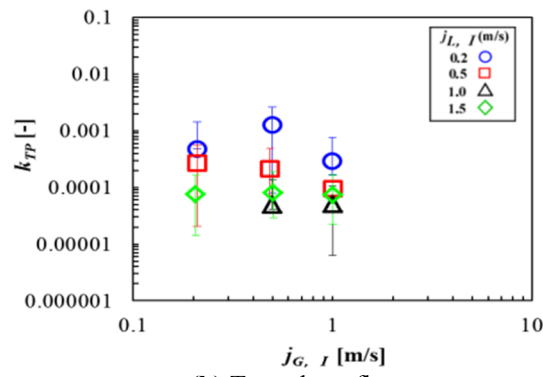
$$\text{Laminar flow region } (Re < 2300) \quad k_{SP} = 0.67, \quad (11)$$

$$\text{Turbulent flow region } (Re > 2300) \quad k_{SP} = 291 \times 10^3 Re^{-1.69}. \quad (12)$$

Figure 7 (b) shows the junction loss coefficient for two-phase flow,  $k_{TP}$ , against the volumetric flux of gas in the channel upstream from the junction,  $j_{G,I}$ . It can be seen that the loss coefficient for two-phase flow is nearly constant at 0.0001, independent of  $j_{G,I}$  and  $j_{L,I}$  except for in annular flows. The data at  $j_{L,I} = 0.2$  m/s seem to be inaccurate because  $P_{d,TP}$  data become small with decreasing of  $j_{L,I}$ .



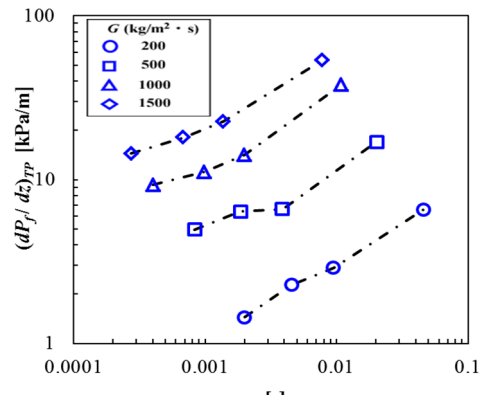
(a) Single-phase flow



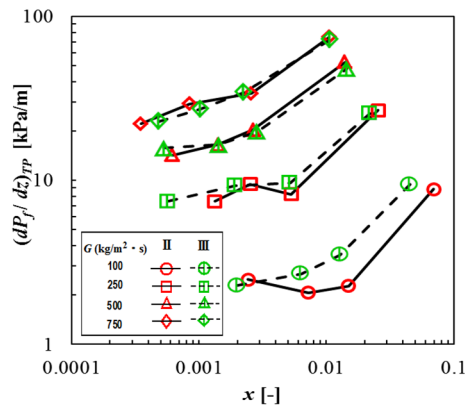
(b) Two-phase flow

Fig. 7: Y-junction loss coefficient

Figures 8 (a) and (b) show the present two-phase frictional pressure drop data for the channels upstream and downstream from the junction,  $(dP_f/dz)_{TP}$ , against the mass quality,  $x$ . In general, the pressure gradient increase with the quality,  $x$ , and total mass flow flux,  $G (= G_L + G_G)$ .



(a) Upstream I



(b) Downstream II, III

**Fig. 8 :** Frictional pressure drop for two-phase flow

The frictional pressure drop data are commonly correlated with the following two-phase friction multiplier,  $\phi_L^2$  (Lochhart & Martinelli, [28]) :

$$\left(\frac{dP_f}{dZ}\right)_{TP} = \phi_L^2 \left(\frac{dP_f}{dZ}\right)_L, \quad (13)$$

where  $\left(\frac{dP_f}{dZ}\right)_L$  is the frictional pressure drop when the liquid flows alone in the same channel. A widely used correlation for the friction multiplier is that proposed by Chisholm and Laird (1958) :

$$\phi_L^2 = 1 + \frac{c}{X} + \frac{1}{X^2}, \quad (14)$$

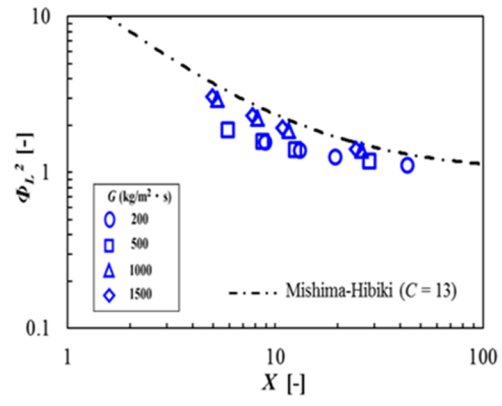
where  $X$  is the Lockhart-Martinelli parameter given by

$$X^2 = \frac{\left(\frac{dP_f}{dZ}\right)_L}{\left(\frac{dP_f}{dZ}\right)_G}, \quad (15)$$

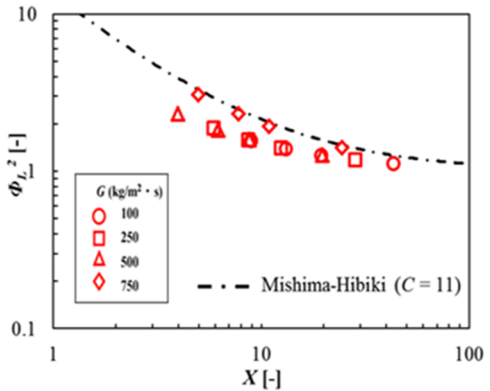
where  $\left(\frac{dP_f}{dZ}\right)_G$  is the frictional pressure drop when the gas flows alone in the same channel. Figures 9 (a) and (b) show the two-phase friction multiplier data against the Lockhart-Martinelli parameter,  $X$ , for the channels upstream and downstream from the junction. The dot-dashed line is the calculated curve by Mishima-Hibiki [29], who proposed the  $C$  correlation as follows :

$$C = 21(1 - e^{-0.319D_H}). \quad (16)$$

where  $D_H$  is the hydraulic diameter of the channel. Here, the unit of  $D_H$  should be in millimeter. The data are well correlated with the Lockhart-Martinelli parameter, and is a little bit lower than the calculation by Mishima-Hibiki [29].



(a) Upstream I



(b) Downstream II, III

**Fig. 9 :** Two-phase frictional multiplier data against Lockhart & Martinelli parameter

### 3.4. Bubble velocity

Figure 10 shows the bubble velocity data,  $u_G$ , for the respective channels in the present experiment against the total volumetric flux of gas and liquid,  $j_G + j_L$ . The solid line of  $u_G = j$  is applicable to homogenous flows. It can be seen the data agree reasonably with  $u_G = j$ . Figure 11 shows a comparison of the bubble velocity between experiment and calculation by the drift flux model of Zuber and Findlay [30] :

$$u_G = C_0 j + V_{Gj} \quad (17)$$

Here,  $V_{Gj}$ , is the drift velocity, was taken as zero because of horizontal flow. The distribution parameter,  $C_0$ , was determined by Kawahara et al.'s correlation [31] :

$$C_0 = \alpha B_o^{0.19} Re_L^{-0.01} We_G^{0.01} \quad (18)$$

and the distribution parameter,  $C_0$ , in this study are proposed :

$$C_0 = 1.02 B_o^{0.19} Re_L^{-0.01} We_G^{0.01} \text{ for upstream I } (D_H = 3.24 \text{ mm}) \quad (19)$$

$$C_0 = 1.82 B_o^{0.19} Re_L^{-0.01} We_G^{0.01} \text{ for downstream II and III } (D_H = 2.43 \text{ mm}) \quad (20)$$

In Eqs. (19) and (20),  $B_o$  is the Bond number,  $Re_L$  the liquid Reynolds number and  $We_G$  the gas Weber number. As seen in Fig. 11, the calculations agree well with the data within root mean square errors of 15% for both the upstream and the downstream channels.

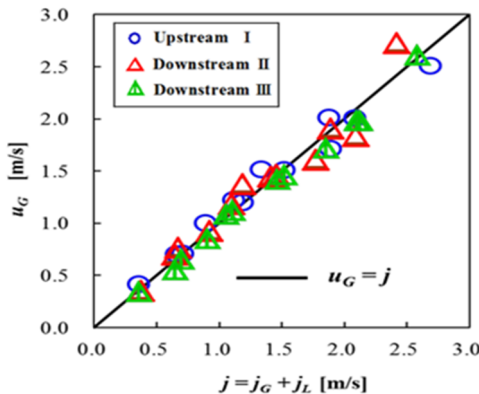


Fig. 10 : Bubble velocity data

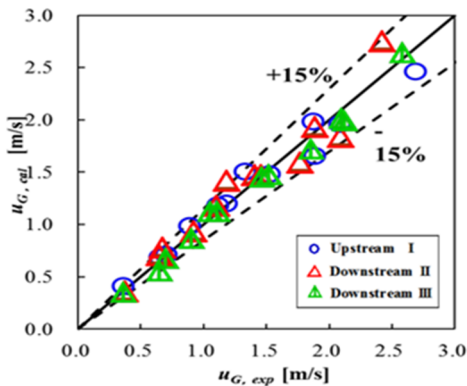


Fig. 11 : Comparison of bubble velocity between experiment and calculation

### 3.5. Bubble length

Figure 12 shows the bubble length data divided by the channel width,  $L_G/w$ . The abscissa is the ratio of the gas volume flow rate to the liquid one,  $Q_G/Q_L$ . The solid curve represents calculation by Garstecki et al.'s correlation [32] :

$$\frac{L_G}{w} = 1 + \frac{Q_G}{Q_L} \quad (21)$$

whereas the dashed lines represents the calculation by Miyagawa's correlation [33] :

$$\frac{L_G}{w} = \left(1 + \frac{Q_G}{Q_L}\right) \times 5 \quad (22)$$

The data for both the upstream and the downstream channels have a similar trend to both the solid curve and the dashed curve, however it approaches to the value calculated by Miyagawa's correlation as  $Q_G/Q_L$  increases.

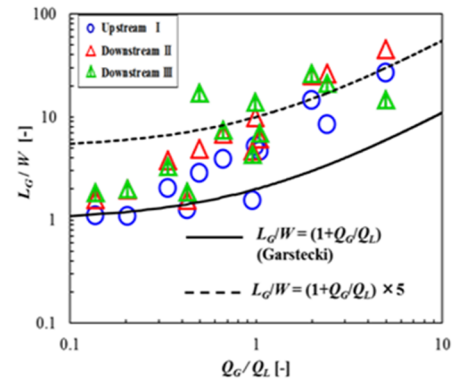


Fig. 12 : Dimensionless bubble length data against gas-liquid volume flow rate ratio in the upstream and the downstream channels

Figure 13 shows the ratio of bubble length,  $L_G$ , to unit cell length,  $L$  ( $= L_G + L_L$ ;  $L_L$  is the liquid slug length) against homogeneous void fraction  $\beta$  ( $= j_G/(j_G + j_L)$ ) in the upstream and the downstream channels. The solid curve shows the calculation by Kawahara et al.'s correlation [34] :

$$\frac{L_G}{L} = \frac{0.9\beta^{0.68}}{1 - 0.1\beta^{0.005}} \cong \beta^{0.68} \quad (23)$$

Eq. (23) was proposed based on the data for horizontal straight microchannels with square and circular cross-sections. The  $L_G/L$  data for both the upstream and downstream channels distribute around the curve. Therefore the junction does not affect  $L_G/L$  data, the Kawahara et al.'s correlation can be applied, irrespective of the channel geometry.

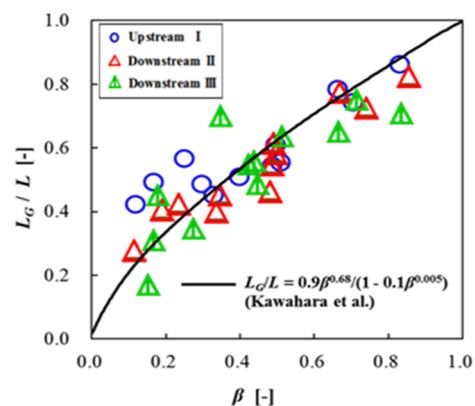
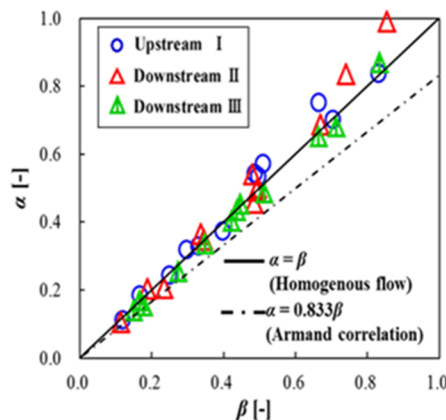


Fig. 13 : Length ratio of large gas bubble to unit cell against homogenous void fraction

### 3.6 Void fraction

Figure 14 shows the void fraction data,  $\alpha$ , in the present experiment against the homogeneous void fraction,  $\beta = j_G/(j_G + j_L)$ . The solid line of  $\alpha = \beta$  is applicable to homogeneous flow, and the dashed lines represents the Armand's correlation [35],  $\alpha = 0.833\beta$ . The void fraction,  $\alpha$ , data especially for downstream III case, agree reasonably with the homogeneous flow. Almost all the data are higher than Armand's correlation.



**Fig. 14 :** Void fraction against homogeneous void fraction

## IV. CONCLUSIONS

Water single-phase flow and air-water two-phase flow experiments were conducted at room temperature and at near atmospheric pressure using a horizontal rectangular minichannel with Y-junction. The width ( $W$ ), the height ( $H$ ) and the hydraulic diameter ( $D_H$ ) for the upstream channel from the junction were 4.60 mm, 2.50 mm and 3.24 mm, while those for the downstream channel were 2.36 mm, 2.50 mm, 2.43 mm. The main findings can be summarized as follows:

- Two type of flow patterns, i.e., slug flow and annular flow are observed under the present flow conditions.
- The junction pressure loss coefficient in the single-phase laminar is constant independent of Reynolds number, but decreases with increasing of it in turbulent flow. The coefficient in two-phase flow is nearly constant, independent of  $j_L$  and  $j_G$  except for in annular flows.
- Frictional pressure drop for two-phase flows,  $(dP_f/dz)_{TP}$ , increases with the mass quality at a fixed mass flow flux,  $G$ , for both the upstream and the downstream channels from the junction. In addition,  $(dP_f/dz)_{TP}$  increases with  $G$  at a fixed mass quality.
- Two-phase frictional pressure drop data are a little bit lower than the calculation by the

Chisholm and Laird correlation with Mishima-Hibiki's correlation.

- The bubble velocity data,  $u_G$ , for both the upstream and the downstream channels agree reasonably with that calculated by homogenous flow model. The data were well correlated with the drift flux model with Kawahara et al.'s modified  $C_0$  parameter correlation.
- The bubble length data,  $L_G$ , for both the upstream and the downstream channels have a similar trend to both the Garstecki et al.'s correlation and Miyagawa's correlation, however it approaches to a value calculated by Miyagawa's correlation as  $Q_G/Q_L$  increases.
- The ratio of bubble length to unit cell length data,  $L_G/L$ , can be predicted by the Kawahara et al.'s correlation, irrespective of channel aspect ratio.
- The void fraction data,  $\alpha$ , especially for downstream III case, agree reasonably with those for homogeneous flow.

## Acknowledgements

The authors deeply appreciate DIKTI of Indonesian government and State Polytechnic of Cilacap for the fellowship and the permission to Mr. Agus Santoso to study in Kumamoto University.

## REFERENCES

- [1] Elazhary, A.M. & Soliman, H.M, Two-phase flow in a horizontal mini-size impacting T-junction with a rectangular cross-section, *International Journal of Multiphase flow*, 42, 2012, 104-114.
- [2] Elazhary, A. M. & Soliman, H. M., Single- and two-phase pressure losses in a horizontal mini-size impacting tee junction with a rectangular cross-section, *Experimental Thermal and Fluid Science*, 4, 2012, 67-76.
- [3] Tsuyama, M. & Taga, M., On the flow of the air-water mixture in the branch pipe, *Bulletin JSME*, 2, 1959, 151-156.
- [4] Mohamed, M.A., Soliman, H.M. & Sims, G.E., Conditions for complete phase separation in an impacting tee junction at various inclinations of the outlet arms, *International Journal of Multiphase Flow*, 47, 2012, 66-72.
- [5] Mohamed, M.A., Soliman, H.M. & Sims, G, Effects of pipe size and system pressure on the phase redistribution, *Experimental Thermal and Fluid Science*, 54, 2014, 219-224.
- [6] Chen, J., Wang, S., Ke, H., Zhou, M. & Li, X., Experimental investigation of annular two-phase flow splitting at a micro impacting T-junction, *Chemical Engineering Science*, 118, 2014, 154-163.

- [7] Chen, J., Wang, S., Zhang, X., Ke, H. & Li, X., Experimental investigation of two-phase slug flow splitting at a micro impacting T-junction, *International Journal of Heat and Mass Transfer*, 81, 2015, 939-948.
- [8] El-Shaboury, A.M.F., Soliman, H.M. & Sims, G.E., Two-phase flow in a horizontal equal-sided impacting tee junction, *International Journal of Multiphase Flow*, 33, 2007, 411-431.
- [9] Stacey, T., Azzopardi, B.J. & Conte G., The split of annular two-phase flow at a small diameter T-junction, *International Journal of Multiphase Flow*, 26, 2000, 845-856.
- [10] Tae, S. J. & Cho, K., Two-phase flow distribution and phase separation through both horizontal and vertical branches, *KSME International Journal*, 17(8), 2003, 1211-1218.
- [11] Tae, S. J. & Cho, K., Two-phase split of refrigerants at a T-junction, *International Journal of Refrigeration*, 29, 2006, 1128-1137.
- [12] Wren, E., Baker, G., Azzopardi, B.J. & Jones, R., Slug flow in small diameter pipes and T-junctions, *Experimental Thermal and Fluid Science*, 29, 2005, 893-899.
- [13] Das, G., Das, P.K. & Azzopardi, B.J., The split of stratified gas-liquid flow at a small, *International Journal of Multiphase Flow*, 31, 2005, 514-528.
- [14] Yang, L. & Azzopardi, B.J., Phase split of liquid-liquid two-phase flow at a horizontal T-junction, *International Journal of Multiphase Flow*, 33, 2007, 207-216.
- [15] Ling-yang, W., Ying-xiang, W., Zhi-chu, Z., Jun, G., Ju, Z. & Chi, T., Oil-water two-phase flow inside T-junction, *Journal of Hydrodynamics*, 20(2), 2008, 147-153.
- [16] Azzi, A., Al-Attiyah, A., Qi, L., Cheema, W. & Azzopardi, B.J., Gas-liquid two-phase flow division at a micro-T-junction, *Chemical Engineering Science*, 65, 2010, 3986-3993.
- [17] He, K., Wang, S. & Huang, J., The effect of surface tension on phase distribution of two-phase flow in a micro-T-junction, *Chemical Engineering Science*, 66, 2011, 3962-3968.
- [18] Wang, S., He, K. & Huang, J., Phase splitting of a slug-annular flow at a horizontal micro-T-junction, *International Journal of Heat and Mass Transfer*, 54, 2011, 589-596.
- [19] Reis, E.D. & Goldstein Jr, L., Fluid dynamics of horizontal air-water slug flows through a dividing T-junction, *International Journal of Multiphase Flow*, 50, 2013, 58-70.
- [20] Ishiguro, K., Iguchi, M., Mizuno, Y. & Terauchi, Y., Separation of gas from downward gas-liquid two-phase flow using a Y-junction of poor wettability, *JSME International Journal, series B* 47(11), 2004, 795-802.
- [21] Guangbin, D., Zongming, L., Guangli, C., Shougen, H. & Jun, Z., Experimental investigation of gas-solid two-phase flow in Y-shaped pipeline, *Advanced Powder Technology*, 21, 2010, 468-476.
- [22] Chen, J., Wang, S., Ke, H., Cai, S. & Zhao, Y., Gas-liquid two-phase flow splitting at microchannel junctions with different branch angles, *Chemical Engineering Science*, 104, 2013, 881-890.
- [23] Calvanti, W.S., Belem, E. Z. G., De Lima, W. C. P. B., Calvante, F. P., Barbosa, S. R., Neto, S. R. F. & de Lima, A. G. B., Non-isothermal three-phase flow of petroleum, gas and water in T and Y junctions, *International journal of modeling and simulation for petroleum industry*, 5(1), 2011, 43-52.
- [24] Singh, B., Singh, H. & Sehgal, S. S., CFD Analysis of fluid flow parameters within a Y-shaped branched pipe, *International Journal of Latest Trends in Engineering and Technology*, 2(2), 2013, 313-317.
- [25] Hirani, A. A. & Kiran, C. U., CFD simulation and analysis of fluid flow parameters within a Y-Shaped Branched Pipe, *IOSR Journal of Mechanical and Civil Engineering*, 10(1), 2013, 31-34.
- [26] Zhong, H., Wang, X. P., Salama, A. & Sun, S., Quasistatic analysis on configuration of two-phase flow in Y-shaped tubes, *Computers and Mathematics with Applications*, 68, 2014, 1905-1914.
- [27] Shah, R. K. & London, A. L., *Laminar flow forced convection in ducts* (Academic Press, New York, 1978)
- [28] Lockhart, R. W. & Martinelli, R. C., Proposed Correlation of Data for isothermal Two-Phase, Two-Component Flow in Pipes, *Chem. Eng. Progress*, 45, 1949, 38-48.
- [29] Mishima, K. & Hibiki, T., Some characteristics of air-water two-phase flow in small diameter vertical tubes, *International Journal Multiphase Flow*, 22(4), 1996, 703-712.
- [30] Zuber, N. & Findlay, J.A., Average volumetric concentration in two-phase flow system, Trans, *ASME J. Heat Transfer* 87, 1968, 453-468.
- [31] Kawahara, A., Sadatomi, M., Nei, K. & Matsuo, H., The characteristics of two-phase flow in rectangular micro channel with a T-junction type gas-liquid mixer, *Heat Transfer Engineering*, 32, 2011, 585-594.
- [32] Garstecki, P. et al., Formation of droplets and bubbles in a micro fluidic T-junction-scaling

- and mechanism of break-up, *Lab on a Chip*, 6(2), 2006, 437-446.
- [33] Miyagawa, S., *Study on characteristics of gas-liquid two phase flow through singularities*, Kumamoto University Master Thesis, 2014.
- [34] Kawahara, A., Sadatomi, M. & Shimokawa, S., Lengths of bubble and slug and pressure drop in gas-liquid slug flow in micro channels, *Multiphase Science and Technology*, 24(3), 2012, 239-256.
- [35] Armand, A. A., The resistance during the movement of a two-phase system in horizontal pipes, *Izvestia Vses. Teplotekh. Inst.*, 1, (AERE-Lib/Trans 828), 1946, 16-23.